5 Meson Spectroscopy at LEAR with the Crystal Barrel

M. Heinzelmann and C. Amsler

in collaboration with:
Academy of Science (Budapest); Universities of Bochum, Bonn, Hamburg, Karlsruhe, München, Paris VI; CERN; Carnegie Mellon University; CRN-Strasbourg); RAL; UC-Berkeley

(CRYSTAL BARREL COLLABORATION).

The Crystal Barrel detector was dismantled at the end of 1996, following the closure of the Low Energy Antiproton Ring. Our activities were completed with the submission of the last two theses [1, 2]. For full details on the results achieved with Crystal Barrel, we refer to previous annual reports and to a review article [3].

5.1 Annihilation at 900 MeV/c

In 2000 we finalized the analysis of $\bar{p}p$ annihilation in flight at 900 MeV/c into three neutral pseudoscalars, $\pi^0\pi^0\pi^0$, $\pi^0\pi^0\eta$ and $\pi^0\eta\eta$, leading to six detected photons [2, 4]. We were motivated by a search for radial excitations of scalar and tensor mesons, and also by the controversy around the quark content of the $f_0(1710)$ [5, 6, 7]. The analysis is based on 17.9 million events which were taken with the all-neutral trigger during the last data taking run of Crystal Barrel at LEAR. The offline analysis required complete reconstructed events with exactly six clusters and no charged tracks.

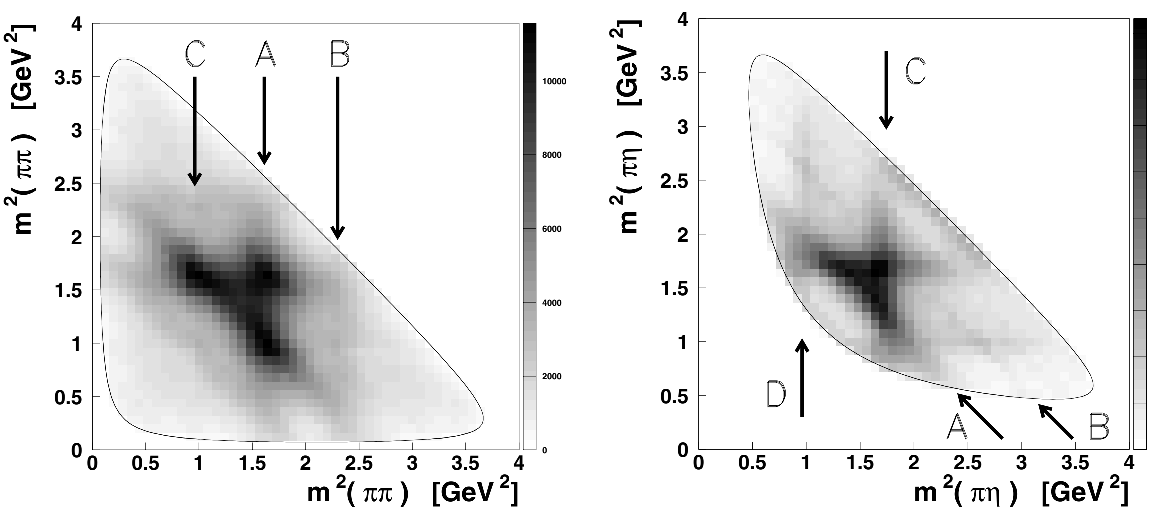

Figure 5.1: *Left: Dalitz plot for* $\bar{p}p \to \pi^0\pi^0\pi^0$ *(six entries per event) with* $f_2(1270)$ *(A),* $f_0(1500)$ *(B),* $f_0(980)$ *(C). Right: Dalitz plot for* $\bar{p}p \to \pi^0\pi^0\eta$ *(two entries per event) with* $f_2(1270)$ *(A),* $f_0(980)$ *(B),* $a_2(1320)$ *(C) and* $a_0(980)$ *(D).*

The three annihilation channels were selected by applying kinematic fits requiring also three pairs of 2γ invariant masses to match the π^0 or η masses. For measurements in flight the annihilation vertex of neutral events was not observed and had therefore to be determined by the kinematic fit. The feedthrough from one channel to the other was determined to be less than 0.7 %. The reaction $\bar{p}p \to \omega\pi^0$ ($\omega \to \pi^0\gamma$), with a missing γ, was the dominating background channel for $\pi\eta\eta$ and $\pi^0\pi^0\eta$. Background contributions of 13 % and 3 %, respectively, were estimated from the data. This background was simulated and taken into account in the partial wave analysis. The background in the $3\pi^0$ channel was negligible.

We obtained 600,962 $3\pi^0$, 161,158 $\pi^0\pi^0\eta$ and 18,419 $\pi^0\pi^0\eta$ events with a detection and reconstruction efficiency of about 27 %.

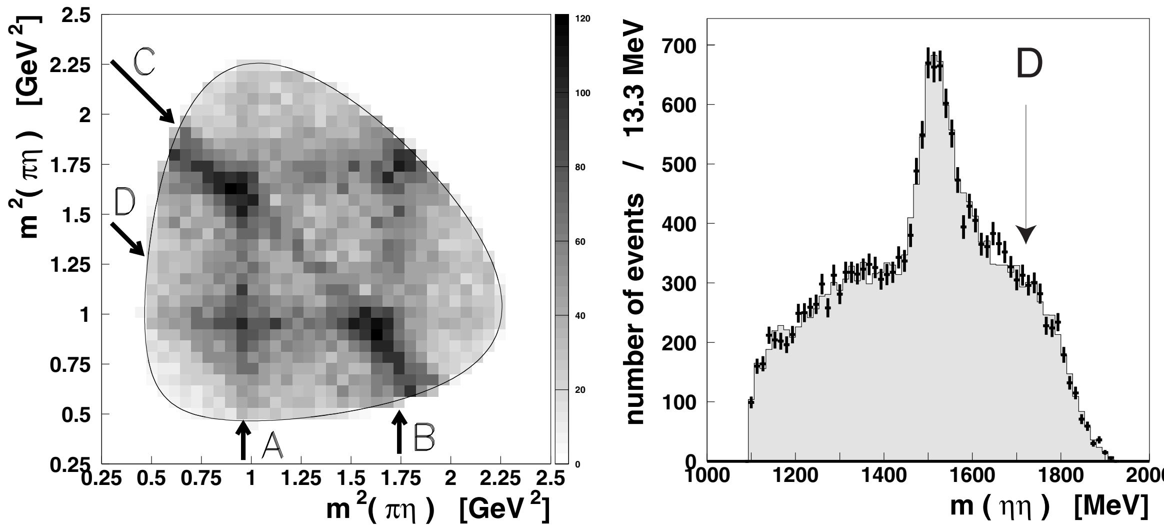

Figure 5.2: *Left: Dalitz plot for $\bar{p}p \to \pi^0\eta\eta$ (two entries per event) with $a_0(980)$ (A), $a_2(1320)$ (B), $f_0(1500)/f_2'(1525)$ (C). The arrow D shows the expected location of the relatively narrow $f_0(1710)$. Right: $\eta\eta$ mass projection showing the $f_0(1500)/f_2'(1525)$. The long tail is due to the new $f_2(1870)$. The shaded histogram is the fit discussed in the text.*

The symmetrised $3\pi^0$ Dalitz plot is shown in Fig. 5.1 (left). One observes the $f_2(1270)$ and $f_0(1500)$. A faint dip in the 1500 MeV band around 1000 MeV corresponds to the $f_0(980)$ interfering destructively with the structure at 1500 MeV. Figure 5.1 (right) shows the Dalitz plot for $\pi^0\pi^0\eta$. One observes the $f_2(1270)$, $f_0(980)$, $a_2(1320)$ and $a_0(980)$. The symmetrised $\pi^0\eta\eta$ Dalitz plot and the $\eta\eta$ mass projection are shown in Fig. 5.2. One observes the $a_2(1320)$, $f_0(1500)/f_2'(1525)$ and a band around 1000 MeV from the $a_0(980)$. In the region of the $f_0(1710)$, only the interference of the two $a_0(980)$ bands can be observed and no signal is present (arrow D).

5.2 Analysis and results

An amplitude analysis of the above Dalitz plots (based on the K-matrix formalism) was performed. While annihilation at rest in liquid hydrogen proceeds mainly from S-states (J=0 or 1), more initial states are contributing with increasing energies. The $J = 4$ contributions to the data sets was found to be less than 5 % and contributions from $J \geq 4$ were therefore neglected. The following initial partial waves were included in the analysis of the present data: ${}^1S_0$, ${}^3P_1$, ${}^3P_2 + {}^3F_2$, ${}^1D_2$, and ${}^3F_3$. Since there are four independent kinematic variables, we performed a maximum likelihood fit. The $\pi\pi$, $\pi\eta$ and $\eta\eta$ S-waves were described with our parameterization from the at rest data [8]. To fit the $3\pi^0$ and $\pi^0\eta\eta$ data sets the program was ported to the NEC SX-5 supercomputer of the Swiss CSCS facility in Manno. A typical fit took about 10 hours.

The description of $\pi^0\pi^0\eta$ requires, apart from the resonances seen directly in Fig. 5.1, a 2^{++} isovector state with mass and width

$$M = 1698 \pm 44 \text{ MeV}, \ \Gamma = 265 \pm 55 \text{ MeV}, \tag{5.1}$$

in excellent agreement with our result for the $a_2(1660)$ in $\pi^0\eta\eta$ at 1940 MeV/c [9]. This is the radial excitation of $a_2(1320)$. The L3 collaboration also reports a 2^{++} state in this mass region in $\gamma\gamma$ interactions, decaying into $\pi^+\pi^-\pi^0$ [10].

The description of the $3\pi^0$ data requires, apart from the obvious resonances directly seen in Fig. 5.1, a new broad tensor state with a mass of 1877 $\pm$ 30 MeV and a width of 318 $\pm$ 55 MeV, decaying into $\pi\pi$, which we call $f_2(1870)$. This state is also required in the analysis of the $\pi^0\eta\eta$ data, where it decays into $\eta\eta$. The $3\pi^0$ and $\pi^0\eta\eta$ data sets were therefore fitted simultaneously with a common description of the resonances. The fit differs only marginally from the ones obtained by the single fits.

The results of the coupled fit for tensor resonances are shown in Table 5.1. The mass and width of the $f_2'(1525)$ agree well with the known values. The $f_2(1565)/AX$, discovered in our earlier ASTERIX experiment [11], is seen here for the first time in annihilation in flight.

Table 5.1: *T-matrix pole parameters of the $\pi\pi$ and $\eta\eta$ D-waves of the coupled fit. The $f_2(1270)$ parameters are fixed.*

	Mass [MeV]	Width [MeV]
$f_2(1270)$	1275	185
$f_2'(1525)$	1508 $\pm$ 9	79 $\pm$ 8
$f_2(1565)$	1552 $\pm$ 13	113 $\pm$ 23
$f_2(1870)$	1867 $\pm$ 46	385 $\pm$ 58

The $f_2(1870)$ is new. The ratio of $\eta\eta$ to $\pi^0\pi^0$ branching fractions is 0.27 $\pm$ 0.10. This ratio is related to SU(3) mixing angles and one gets two solutions for the mixing angle [2], one being compatible with a pure $\bar{u}u + \bar{d}d$ state, hence a radial excitation of the $f_2(1270)$. Then $f_2(1565)$ and $f_2(1870)$ are both radial excitations but do not belong to the same nonet. The other solution leads to a large $\bar{s}s$ component for $f_2(1870)$, in which case $f_2(1565)$ $a_2(1660)$ and $f_2(1870)$ would belong to the same nonet of radially excited 2^{++} $q\bar{q}$ mesons. The ambiguity could be solved by measuring the $f_2(1870)$ decay rates into $\eta\eta$ or $K\bar{K}$.

Figure 5.3 shows the $\pi^0\pi^0$ and $\pi^0\eta$ mass projections for $3\pi^0$ and $\pi^0\pi^0\eta$. The long tails are due to the two new tensor mesons $f_2(1870)$ and $a_2(1660)$.

Table 5.2: *Tentative SU(3) assignment of scalar mesons. The first isoscalar (second column) couples strongly to pions, the second (third column) strongly to kaons. The "pionic" states are very broad, except $f_0(1500)$, which is supernumerary.*

$I=1$	$I=0$	$I=0$	$I=1/2$	Nature
$a_0(980)$	$f_0(400-1200)$ (or σ)	$f_0(980)$	$\kappa(900)$	Scattering resonances
$a_0(1450)$	$f_0(1370)$ $f_0(1500)$	$f_0(1710)$	$K_0^*(1430)$	$1^3P_0(q\bar{q})$
?	$f_0(2020)$	$f_0(2200)$	$K_0^*(1950)$	$2^3P_0(q\bar{q})$

The $\eta\eta$ mass projection for $\pi^0\eta\eta$ is shown in Fig. 5.2 above. The data description is good and there are no significant deviations. The inclusion of an $f_0(1710)$ in either the $\eta\eta$ or the $\pi\pi$ S-wave was not successful. The $f_0(1710)$ is therefore not required to describe the data at 900 MeV/c. This is not suprising if this state is $\bar{s}s$, as the OZI rule forbids the production of $\bar{s}s$ states in $\bar{p}p$ annihilation. Recent results in central production [12] show that, indeed, this state prefers to decay into $K\bar{K}$ rather than into $\pi\pi$ which therefore suggests that this

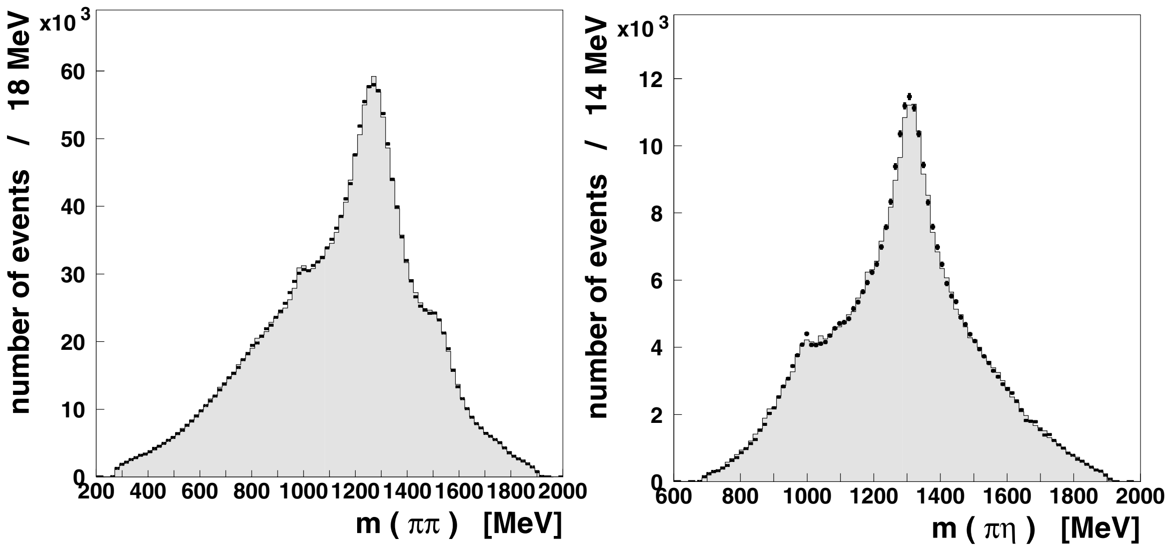

Figure 5.3: *Left:* $\pi^0\pi^0$ *mass projection in the* $3\pi^0$ *channel. The shaded histogram shows the best fit. The peaks are due to* $f_0(980)$, $f_2(1270)$ *and* $f_0(1500)/f_2(1565)$, *and the long tail to the new* $f_2(1870)$. *Right:* $\pi^0\eta$ *mass projection in the* $2\pi^0\eta$ *channel. The peaks are due to* $a_0(980)$ *and* $a_2(1320)$, *the tail to* $a_2(1660)$.

meson is the (mainly) $\bar{s}s$ member of the scalar nonet. Our present analysis then strengthens the interpretation of the $f_0(1500)$ as a glueball, or as a state with a large gluonic admixture in its wave-function [13].

Table 5.2 shows a tentative classification of scalar mesons. The low mass scalars are interpreted as scattering resonances. Alternatively, the $a_0(980)$ and $f_0(980)$ are often referred to as $K\bar{K}$ molecules or $q^2\overline{q}^2$ states. For a more detailed discussion and for a bibliography see refs [6, 7].

References

[1] P. Giarritta, PhD Thesis, Universität Zürich (2000)

[2] M. Heinzelmann, PhD Thesis, Universität Zürich (2000)

[3] C. Amsler, Rev. Mod. Phys. 70 (1998) 1293

[4] C. Amsler, Proc. of the Hirschegg 01 Workshop on Hadron Spectroscopy (2001)

[5] C. Amsler, Proc. Workshop on Hadron Spectroscopy, Frascati Physics Series, Vol. XV (1999) p. 609

[6] C. Amsler, Nucl. Phys. A 663 (2000) 93c

[7] C. Amsler in Review of Particle Physics, Eur. Phys. J. C 15 (2000) 682

[8] C. Amsler et al., Phys. Lett. B 355 (1995) 425

[9] A. Abele et al., Eur. Phys. J. C 8 (1999) 67

[10] M. Acciarri et al., Phys. Lett. B 413 (1997) 147

[11] B. May et al., Phys. Lett. B 225 (1989) 450

[12] D. Barberis et al., Phys. Lett. B 462 (1999) 462

[13] C. Amsler and F. E. Close, Phys. Rev. D 53 (1996) 295